Xylene Selectivity at the External Surface of Hierarchical Zeolites: Experiment and Molecular Modeling

Izabel Medeiros-Costa, Catherine Laroche, Benoit Coasne, Javier Pérez-Pellitero

HAL Id: hal-03739170
https://cnrs.hal.science/hal-03739170

Xylene Selectivity at the External Surface of Hierarchical Zeolites: Experiment and Molecular Modeling

Izabel C. Medeiros-Costa[†], Catherine Laroche[†], Benoit Coasne[‡], Javier Pérez-Pellitero[†,*]

[†] IFP Energies nouvelles, Rond-point de l'échangeur, BP3, 69360 Solaize, France

[‡] Univ. Grenoble Alpes, CNRS, LIPhy, F-38000 Grenoble, France

*E-mail address: javier.perez-pellitero@ifpen.fr (J. Pérez-Pellitero)

ABSTRACT. Hierarchical faujasite zeolites made up of nanoparticle aggregates (NA) and layer-like structures (LL) are evaluated for xylene adsorption in both gas and liquid phases. For NA zeolites, several samples with varying external surfaces and meso/macropore volumes are considered. Compared to conventional faujasite, xylene adsorption isotherms as measured by means of thermogravimetric experiments display higher adsorption capacities for the NA faujasites. This adsorption capacity increase is found to be linked to the zeolite external surface area. However, in the case of the LL zeolite, despite its large external surface, the xylene adsorption capacity is found to be similar to that of the conventional zeolite. With all hierarchical samples, the paraxylene selectivity assessed through batch adsorption experiments in liquid phase are smaller than the selectivity observed for the conventional zeolite. The observed selectivity decrease seems to be associated with the decrease in functional window adsorptive sites when enhancing the external surface. To shed light on the observed phenomenon, Monte Carlo simulations in the Grand Canonical ensemble are performed to investigate the adsorption of xylene in a bulk infinite zeolite and a zeolite sample exhibiting an external surface. For the latter sample, the external surface chosen is made up of incomplete cavities and, therefore, defective window sites. In agreement with our experiments, the results from molecular simulation indicate a selectivity loss associated with the sample large external surface.

KEYWORDS. Hierarchical zeolites, surface, adsorption, separation, selectivity, xylenes

1. Introduction

Xylene separation is a process of great importance in the chemical industry. In particular, among the different isomers (paraxylene px, metaxylene mx and orthoxylene ox), paraxylene px is the most used isomer in the petrochemical industry. When considering separation using porous adsorbents, the xylene separation efficiency is governed by a set of various adsorbent properties (mainl adsorption capacity, diffusion time, and selectivity) which strongly depend on the type of adsorbent considered. In practice, the adsorbents targeted for xylene separation are based on microporous zeolite of the type faujasite. Several forms of this zeolite present interesting selectivities towards paraxylene (owing to confinement in their microporosity) but the access time through diffusion within their porosity is an important parameter that must be improved [1,2]. To improve such transport aspects in xylene separation, hierarchical faujasite zeolites are often seen as promising materials (see Refs. [3–8] for different types of hierarchical zeolites that can be synthesized such as nanosized zeolites and mesoporous zeolites). While such hierarchical samples are known to lead to greatly improved transport properties for catalytic and adsorption processes [9–15], the existence of a very large external surface area – inherent to their hierarchical porosity – raises questions regarding its impact on these processes. To provide insights into this question, we report here a combined experimental and molecular simulation study on xylene adsorption in hierarchical faujasite zeolites including at their external surface.

To assess the role of the outer surface on xylene selectivity, the selection of appropriate methods to probe xylene adsorption is also an essential step to carry out. In the literature, the study of xylene adsorption has been considered extensively in both gas and liquid phases. In particular, an

important number of studies has reported thermogravimetry assessment of xylene adsorption and diffusion from the gas phase [16–22]. Upon applying well-controlled temperature and partial pressure conditions, the adsorbed fluid mass in the zeolite can be measured using a thermobalance either at equilibrium or as a function of time (by following the system's dynamic response to a given perturbation). Using thermogravimetric analyses, xylene adsorption can be performed under various conditions to obtain adsorption isotherms and isobars. As a consequence isosteric enthalpies of adsorption are also accessible by means of this technique [23].

As an example of themogravimetric analysis applied to xylenes, Bellat and coworkers investigated the xylene adsorption at the external surface of Y-type faujasite zeolites and determined the adsorption isotherms for the *px* and *mx* isomers at 25°C [24]. In order to disentangle adsorption at the outer surface from that occurring within the micropores, a simple model was used. This model correlates linearly the adsorbed mass to the film thickness *t* adsorbed film at the surface of a reference (alumina) material. The results by Bellat et al. suggest that xylene adsorption corresponds to ~3.5 molecules/α cage and that *mx* adsorption at the surface is more important that *px* adsorption. This indicates that the zeolite external surface is selective towards the most polar isomer (*mx*). Thermogravimetry was also used to further investigate xylene coadsorption in a BaX zeolite. To do so, an advanced set-up system was used by coupling the gas outlet to a chromatograph [25]. By means of this technique, the selectivities was measured as a function of the xylene loading inside the adsorbent. Above 2 molecules/α cage, *px* selectivity is observed. Using differential calorimetry, the adsorption of xylene isomers was also investigated for the BaX zeolite [25]. The measured enthalpies of adsorption were found to be almost constant as a function

of loading until the complete filling of the α cages. At this point, the adsorption heat rapidly diminishes towards the heat of vaporization for the pure xylene isomers.

When considering liquid phase experimental techniques, two main techniques have been previously employed. In the case of liquid batch experiments, the porous solid is set in contact with a liquid and then exposed to a specific adsorbate concentration [26–28]. By exploiting the changes in the liquid phase composition experienced during the equilibration of the adsorption process, one can measure the adsorbed amount in the sample but also its selectivity. Using breakthrough experiments, one can also characterize the adsorbent by determining its adsorption capacity and selectivity. Such experiments, which involve similar principles to liquid phase chromatography, have been employed to assess porous solids towards xylene separation [29–32]. Although the use of the breakthrough technique allows obtaining key information on separation and mass transfer capacities, the main inconvenient is the need for a large quantity of solid sample (which may represent an obstacle in many cases).

The production of hierarchical zeolite samples usually involves a large increase in their outer surface area. The role of such an important external surface on the separation of xylenes remained to be fully explored. In this context, using different hierarchical zeolites, the goal of the present work is to address the impact of the external surface but also of the different porosities on xylene adsorption. Using well-characterized hierarchical zeolites [33], we consider two types of BaX faujasite hierarchical zeolites made of nanoparticles: (1) nanoparticle aggregates (NA) and (2) layer-like arrangements (LL). The NA samples are obtained by aggregating crystals with

mesoporosity formed in between them. The LL sample, which consists of self-assembled faujasite layers, contains both inter and intra-layer meso/macropores. By combining gas phase thermogravimetry and liquid batch experiments with a molecular modeling approach, we aim at assessing xylene adsorption on hierarchical zeolites. While thermogravimetry allows measuring the adsorption isotherms and, subsequently, deriving the corresponding isosteric adsorption enthalpies, batch experiments are well suited to measure xylene adsorption selectivities in both hierarchical and conventional BaX zeolites. Although these quantities are macroscopic parameters, they are expected to provide key information about the interaction between xylene isomers and the zeolite outer surface. In parallel, Grand Canonical Monte Carlo (GCMC) molecular simulations provide a microscopic understanding of xylene separation in hierarchical zeolites. In particular, using this atom-scale numerical method, the impact of the zeolite external surface on the xylene adsorption selectivity will be studied. The details of the experimental and theoretical techniques employed to investigate xylene adsorption are introduced in the experimental and computational methods section along with a detailed description of the hierarchical and conventional zeolites tested as adsorbents. The results obtained by means of thermogravimetry and batch experiments are presented in two separate sections: adsorption in partially and fully saturated media. Then, the molecular simulation results are discussed in a section devoted to disentangling surface and bulk contributions to adsorption selectivity. Finally, the conclusion will discuss and summarize our main findings.

2. Experimental

Samples. Nanoparticle Aggregates (NA) and Layer-Like (LL) hierarchical zeolites were tested for xylene adsorption. A full textural characterization of their characteristics can be found in our previous work [33]. The NA zeolites consist of nanoparticles aggregates where both meso/macropores are observed in between the nanoparticles belonging to a given aggregate. Three zeolites from the NA family with different characteristics were considered for the present study. Textural parameters derived from N_2 adsorption are presented in Table 1. Although samples also present macropores, those cannot be measured/quantified by N_2 adsorption, therefore the textural characterization only describes micropore/ mesopore volume and external surface area. The selected zeolites display a microporous volume of about 0.16 cc/g, external surface areas in the range 43-68 m²/g and mesoporous volumes in the range 0.11-0.18 cc/g. The LL zeolite exhibits porosity at both the mesopore and macropore scales. These two porosity types can be coined as intra-layer and inter-layer porosities. The micropore volume for LL zeolite is 0.18 cc/g while the zeolite outer surface area and mesoporous volume are 38 m²/g and 0.08 cc/g, respectively. The domain connectivity between the different porous networks was investigated by means of scanning curves (N_2 adsorption) for both zeolite types (NA and LL). The analysis of the hysteresis loops showed that the meso/macropores are mainly accessible from the outer surface for the NA zeolites. For the LL zeolite, accessibility occurs *via* narrow pores leading to cavitation phenomena. Concerning the surface chemistry analysis, evidence was reported for the presence of a very similar SiOH group density at the outer surface of the different zeolites. For the sake of comparison, a conventional X zeolite with no significant external surface or mesoporosity (microporous volume of 0.25 cc/g) was also used in this work.

Thermogravimetric Analysis. The thermogravimetry experiments were carried out using a thermobalance (SETARAM B 24). This thermobalance is made up of two similar ovens containing each a sample holder. One of the ovens uses reference glass beads while the second oven hosts the zeolite. The experimental set-up is connected to three gas lines. One gas line goes to the top (T) of the balance to avoid damage to the electronic components. Another gas line goes to the so-called reference side (RS). The last gas line is linked to the sample (SS). The latter is connected to a saturator where the carrier gas N_2 gas is in contact with xylene. The temperature of xylene in the saturator is controlled by a heating collar coupled to a thermocouple immersed in liquid xylene. At equilibrium, the partial pressure of px in the carrier gas is assumed to correspond to the px vapor pressure. The saturator also connected to dilution lines that enable mixing the xylene saturated gas with additional nitrogen, therefore enabling us to set different xylene partial pressures. The system is also connected to a flowmeter that controls the gas flow after dilution; this enables varying the xylene partial pressure at constant total flow. Before carrying out the adsorption isotherms measurements, the samples are outgassed by using a heat treatment under N_2 flow which comprises two temperature stages. To prevent degradation of the zeolite, a first slow temperature ramp to 100°C is performed. Then, the temperature is increased until reaching a second dwell at 200 °C where the temperature remains constant for 6 hours. After this outgassing treatment, the temperature is adjusted to start the adsorption experiment. The adsorption isotherms are determined by changing the xylene pressure. For each partial pressure, the system is maintained until equilibrium is reached. The adsorption isotherm is then constructed from the xylene mass adsorbed at a given xylene partial pressure. Single components adsorption isotherms for px and ox were determined at $T = 100$°C, 150°C and 175°C.

Batch Experiments. The xylene liquid adsorption experiments in BaX zeolite were performed by using a 50 cc glass balloon sealed with a rubber stopper and placed on a magnetic stirring plate. The measurement protocol is performed involves three stages. (A) Zeolite and hydrocarbon pretreatment: prior to the experiments, the zeolites are degassed in a vertical quartz tubular furnace. The pretreatment involves a ramp (2°C/min) up to 100°C followed by a dwell at 100°C for 3h. This stage enables us to remove most of water from at low temperature to avoid zeolite degradation. Then, a second temperature ramp (2°C/min) is performed to reach 200°C. The zeolites are then kept for 6 h at 200°C to remove residual water. The pretreatment is done under N_2 flow (20 NL/h). The hydrocarbons are dehydrated prior to experiments by setting them in contact with a 3A zeolite (under stirring at room T) until the water concentration becomes < 15 ppm (as measured by Karl-Fischer titration). (B) Introduction of the zeolite in the balloon, the solvent and the xylenes: after activation, the zeolite powder is put in glass bottles filled with argon and transferred to a glove box to minimize contact with humidity. Around 2.5 g of zeolite is then inserted into the glass balloon (50 cc). Thereafter, about 25 g of normal decane (nC10) are injected in the balloon which is then sealed with a rubber stopper, transferred, and placed under magnetic stirring. Stirring of the mixture in the balloon is carried out for > 30 minutes. Then, a syringe is used to inject around 2.5 g of a xylene mixture (50%:50% *px*/*ox* or *px*/*mx*). The xylene mass is estimated from the mass of the xylene-filled syringe filled and that of the empty syringe after injection. When xylene is added, the timer is started. Sampling was carried out between 5 min and 24 h. For the conventional zeolite, intervals of 20 min until 3h are considered with a last sampling at 24 h. For hierarchical zeolites, sampling is made every 5 min until the first hour with additional measurements at 3 h and 24 h. Sampling is performed by extracting with a syringe an aliquot (whose mass is obtained from the difference between the empty/filled syringe). Upon sampling,

stirring is halted for about 12 seconds to ensure the zeolite powder is decanted at the bottom (so that only liquid is collected). After sampling, the stirring is immediately resumed and the collected aliquots are filtered and transferred into crimp vials. Filtration is achieved using a 200 μm syringe-coupled filter which is employed once per aliquot. This avoids the presence of small zeolite crystals in the solution (not visible). (C) Sample analysis: the filtered aliquots are analyzed using gas phase chromatography. To increase our analysis accuracy, each aliquot was divided to fill two vials.

Molecular Simulation. Surface preparation. In the case of the LL zeolite, some experimental evidence points to a larger amount of the {111} crystal surface [4]. Nevertheless, this fact cannot be generalized to the rest of the considered hierarchical structures. Consequently, the surface direction {011} was selected as cleavage is carried out at the position of the α cages. In this way, it is possible to focus our investigation on the potential impact on *px* selectivity of the generated open cavities at the surface level. Cleavage was carried out using the software Materials Studio [34]. The following parameters were considered: plane of cleavage {hk1} is {011} with an origin (a b c) equal to (0 0 1). The surface reconstruction was performed by considering IR experiments available in our previous work (in which silanol groups were identified at the external surface) [33]. The zeolites exhibit aluminum tetrahedra at the surface so that all missing bonds in the Si or Al tetrahedra were completed with OH groups (such a strategy has been already used in the literature [35,36]). The obtained density of hydroxyl groups was 8 OH/unit cell. After surface generation, the atomic positions at the surface were relaxed (energy minimization) to obtain structures without any electrical dipole moment.

GCMC simulations with a biased insertion strategy for the guest molecules were carried out to determine the adsorption of an xylene isomer equimolar mixture at the surface of a FAU zeolite as well as in the bulk of its porosity. The simulations were carried out using the GIBBS 9.3 code. The xylene molecules were modeled using the electrostatic version of the anisotropic united atom (AUA) for aromatic compounds [37]. To avoid unphysical charge overlap between the aromatic rings and the metallic centers, modifications were considered to distribute the electrostatic interaction around the aromatic ring. The zeolite description was based on a "Kiselev type" potential [38]. All model parameters and method details can be found in the Supporting Information.

3. Results and Discussion

3.1. Xylene Adsorption in Partially Saturated Medium

We evaluate the role of the external surface in hierarchical zeolites on *px* adsorption and selectivity. For this purpose, *ox* isomer was chosen for comparison as it presents greater polarity among the three xylenes, which would possibly facilitate the detection of surface selectivity linked to the difference in polarity of the feed components. In the case of adsorption of pure *px* and *ox*, as performed during the study using thermogravimetry, differences in adsorption enthalpies could be indicative of improved/decreased interaction as a function of the polarity of a given isomer. To assess the adsorption capacity in both conventional and hierarchical zeolites, single component adsorption isotherms for *px* and *ox* were determined using a thermobalance (Fig. 1). Adsorption can be observed even at low xylene pressures. The *px* adsorption in conventional zeolite BaX was

compared with available data in the literature. From Ref. [25], *px* adsorption at 150°C suggests saturation to 3.4 molecules/α cage. In contrast, in the present work, *px* adsorption at the same temperature is about 3.6 molecules/α cage for the conventional zeolite. The origin of the slight difference between the two measurements is believed to be due to different reasons such as the hydration state or the degree of crystallinity of the samples.

When comparing the adsorption capacities of the different samples (Fig. 1), the NA-3 zeolite displays a higher capacity towards adsorption than both the conventional and LL zeolites. Such enhanced capacity is thought to be due with the greater mesoporous volume/external surface area for this sample. This is indeed the main textural difference between the NA-3 and other zeolites considered here. As a result, for the NA-3 zeolite, adsorption most likely corresponds to both micropore filling (around 3.9 molecules/α cage corresponding to the capacity for the conventional zeolite at 100°C) and adsorption in the mesopores/external surface. The last contribution can therefore be assessed from the adsorbed amount difference at saturation and after micropore filling. At 175°C (practical temperature to perform xylene separation), the excess adsorbed amount due to adsorption in mesopores/external surface in the NA-3 zeolite amounts to ~0.4 molecules/α cage. The hierarchical LL zeolite displays *ox* adsorbed amounts matching well those for the conventional sample. On the other hand, *px* adsorption in the LL zeolite is lower than for the conventional zeolite. Two interpretations can be invoked to rationalize these differences: (1) the mesoporous volume in the LL zeolite is too small to lead to non-negligible differences in the overall adsorbed amount or (2) the zeolite morphology for this sample made up of layers has qualitatively modified the nature of the surface. The induced modifications should alter both qualitatively and quantitatively the adsorption properties, i.e. energy and number of adsorbed molecules, at the external surface. In contrast to the conventional zeolite, upon comparing *px* and *ox* adsorption at

saturation, systematically higher adsorbed amounts are found for *ox* in the case of the LL sample. Since this fact implies a modified distribution of the adsorption sites, this observation supports the second hypothesis above. From available data in the literature, an adsorption site referred to as "window site" is often invoked to explain adsorption observed at high filling rates; this site is located at the entrance of the supercages [39,40]. Therefore, xylene adsorption in such a site may be suppressed in the LL zeolite due to the lack of stability caused by the morphology for this sample.

To further analyze and rationalize the measurements obtained by thermogravimetric analysis, different thermodynamic adsorption models were implemented. These models allow validating the thermodynamic consistency of the measurements. By means of Polanyi's adsorption potential theory, the adsorption isotherms obtained at various temperatures were plotted using the following characteristic curve [41]:

$$A = f(W) = RT \ln p_{sat}/p \qquad (1)$$

where W is the adsorbed amount, A is the adsorption potential, and R the rare gas constant. The adsorption potential theory by Polanyi writes that the adsorption potential is the work exerted by temperature independent adsorption forces [41]. Such a theory proposes that any adsorbent/adsorbate couple can be represented by a specific distribution curve which is independent of temperature: this is the so-called adsorption potential A. Such a characteristic curve was plotted to check the assumption of temperature invariance of the adsorption in both conventional and hierarchical zeolites. As shown in Fig. S1 (a), (b) and (c) in the Supporting Information, for both conventional and hierarchical zeolites, the adsorption of each xylene isomer

measured at different temperatures verifies reasonably this condition. Despite the strong hypotheses in Polanyi's theory, the thermodynamic consistency between the data obtained at different temperatures is an important step as it indicates that the thermobalance measurements are thermodynamically coherent.

Polanyi's theory was employed by Dubinin and Radushkevich to provide a framework to describe adsorption in microporous solids as well as on surfaces. In these extensions, the adsorbed volume distribution is treated as a Gaussian distribution [42]. The Dubinin-Radushkevich (DR) model for adsorption in microporous adsorbents can be expressed in its linear shape: $\ln W = \ln W_0 - B/\beta^2 \, (T \log p_{sat}/p)^2$. By plotting $(T \log p_{sat}/p)^2$ versus the logarithm of the adsorbed volume $\ln W$, the parameter B/β^2 and micropore capacity W_0 can be obtained from the curve slope/intercept. Such fits allow predicting adsorption isotherms at any temperature since these parameters are assumed to be temperature indepedent. The plot of the DR equation shown in Fig. S1(d) and (e) in the Supporting Information is in good agreement with our data for the LL and conventional zeolites. Using the parameters extracted from Fig. S1(d) and (e), the model for *px* and *ox* adsorption isotherms in conventional and LL BaX zeolites can be used satisfactorily (Fig. S2 in the Supporting Information). The model better matches the data for the conventional zeolite than the LL type zeolite, which is believed to be due to the large mesoporosity in the LL zeolite.

In contrast to the conventional and LL zeolites, the NA-3 solid is not well represented by DR equation (restricted to micropore filling). The NA-3 zeolite contains both micro and mesopores, which leads to enhanced *px* and *ox* adsorption compared to the conventional zeolite. As a result,

both adsorption in the micropores and in the mesopores/external surface have to be considered when modeling xylene adsorption in zeolite NA-3. To do so, the micropore volume in zeolite NA-3 was assumed to be the same as in the conventional zeolite. Compared to adsorption in the mesopores/external surface, the adsorbed volume corresponding to microporosity was assumed to coincide to the difference between the total adsorbed amount in NA-3 zeolite and the total adsorbed amount at the same pressure in the conventional sample. After estimating the adsorption volume in the mesopores/external surface, it was described using the characteristic function as defined by Radushkevich: $\log W = \ln W_0 - m/\beta^2 A$ [43]. Such fits for the NA-3 zeolite can be found in Fig. S1(f) of the Supporting Information for each xylene isomer at different temperatures. These parameters provide a means to model adsorption in the mesopores/external surface at different temperatures. Adsorption for the NA-3 hierarchical zeolite can then be expressed by summing adsorption in the micropores in the conventional zeolite and adsorption in the mesopores/external surface. This assumption, which consists of assuming that adsorption in hierarchical materials is the sum of adsorption in the different regions, has been validated for different systems [24,44]. The modelled for adsorption in the NA-3 zeolite, which is shown in Fig. S2, is found to be in good agreement with the experimental data for the different xylene isomers taken at different temperatures.

After calibration of the model parameters for *px* and *ox* adsorption in the conventional and hierarchical zeolites, some key properties such as the heat of adsorption can be derived. The adsorption data in Fig. 1 were determined at different temperatures to derive the enthalpies of adsorption at various adsorbed amounts in the hierarchical and conventional zeolites BaX [23]. In more detail, the isosteric adsorption enthalpies were determined using the Clausius-Clapeyron

equation shown in Equation 2. Such an equation writes that, for a given and constant adsorbed amount θ, the derivative of adsorption pressure with respect to temperature is linked to the isosteric adsorption enthalpy ΔH_{ads}:

$$\frac{\Delta H_{ads}}{R} = [\mathrm{d}\ln p / \mathrm{d}(1/T)]_\theta \tag{2}$$

The isosteric adsorption enthalpies for the hierarchical and conventional zeolites are displayed in Fig. 2. The adsorption enthalpies at 150°C for *px* and *mx* on a conventional BaX zeolite (available from the literature) are also shown in Fig. 2 for comparison [45]. The literature data allows assessing the adsorption enthalpy as a function of the xylene adsorbed amount in presence of isomers other than *px*. As can be seen, larger adsorption enthalpies are found at low adsorbed amounts. At intermediate loadings, the adsorption enthalpies remain almost constant until reaching cage loadings close to 3 which corresponds to fractional loadings higher than 0.85 (the fractional loading is defined as the fraction of porosity filled with respect to complete filling). Across this region (low to intermediate loadings), the behavior of both *px* and *mx* isomers is almost equivalent. In contrast, at high adsorbed amounts, significant drops in the isosteric adsorption enthalpies are found for both isomers. Moreover, when comparing the different isomers, this phenomenon is more pronounced in the case of *px*. This fact indicateds that, close to saturation, the *px* molecules are adsorbed in less energetic sites [45].

The different adsorption measurements performed in this work cover well the medium/high loading region (>3.3 molecules/α cage) where the change of adsorption regime occurs. Then, the impact of the external surface over the adsorption regime may be studied in detail. Contrary to *mx* and *px*, here the difference in the steepness of the curves is less evident [45]. In Fig. 2, we observe that zeolite samples with higher adsorption capacities lead to an offset in the isosteric adsorption

enthalpies which are shifted to larger values (NA-3 > Conv. > LL). A similar behavior is observed for *ox* and *px* isomers. When comparing the adsorption of both isomers, the most compelling situation is found for adsorption in zeolite LL as a higher adsorption enthalpy is found for *ox*. This inversion in the order of adsorption strengths can be rationalized by invoking stronger *ox* adsorption at the LL zeolite external surface. When studying the change in the adsorption enthalpies as a function of the fractional adsorbed amount (i.e. the fraction of porosity filled with respect to full saturation, inset in Fig. 2), very similar behaviors are found for *ox* and *px* isomers.

3.2. Xylene Adsorption in Fully Saturated Medium

We now present the results obtained using liquid batch experiments in terms of *px*/*mx* and *px*/*ox* selectivity for different adsorbed amounts. Such experiments were performed for the conventional and hierarchical BaX zeolites to evaluate the impact on selectivity for each structure type (NA, LL and conventional). Adsorption data for xylene isomers in the different zeolites (as derived from liquid experiments after 3 h and 24 h) are shown in Table 2 and 3. The hierarchical samples after 3h lead to significant amounts of adsorbed xylene which are systematically larger than those for the conventional zeolite. At this stage, the selectivity for the NA-1 and NA-2 hierarchical zeolites are similar and, in some cases, even higher than those for the conventional zeolite. Nevertheless, a loss in selectivity is observed for the NA-3 zeolite (which displays a larger outer surface) and for the LL zeolite. Among these hierarchical zeolites, the latter exhibits the lowest adsorbed amounts.

The adsorption capacity towards xylene at 24 h for the NA-type zeolites remains higher than for the conventional and LL zeolites. The average value (*px*/*mx* and *px*/*ox* taken together) is around

3.13 molecules/α cage in NA zeolites, 2.77 molecules/α cage for conventional zeolite, and 2.57 molecules/α cage for LL. The adsorption capacities as assessed using liquid phase experiments are lower than those measured in gas phase experiments (even if the latter were performed at larger temperatures). These adsorption capacity differences between liquid and gas experiments is thought to be due to diffusional limitations associated to the liquid phase system at low temperatures. This limitation may prevent the zeolitic samples from reaching equilibrium even after 24 h.

As expected, for all cases (*px*/*ox* and *px*/*mx*), *px* adsorption is favorable regardless of the structure type. When comparing the zeolite samples, the largest *px* selectivity is found for the conventional solid. As shown in Table 2 and 3, the selectivities and adsorbed amounts are quite similar as far as *px*/*mx* and *px*/*ox* mixtures for a same zeolite type are concerned; NA-3 displays 3.21 molecule/α cage and *px* selectivity of 1.62 for *px*/*ox* adsorption and 3.07 molecule/α and *px* selectivity of 1.36 for *px*/*mx* adsorption. The larger selectivity difference is obtained for the conventional zeolite which displays a larger lower *px*/*ox* selectivity compared to *px*/*mx* selectivity. The selectivity towards *px* was estimated at different time intervals and, hence, for different adsorbed amounts (Fig. 3). Overall, the observed selectivity trends are similar for the hierarchical and conventional zeolites – except for the last point obtained close to saturation (in this case, the selectivities for the conventional solid are larger than for hierarchical zeolites). Among the different hierarchical zeolites, the zeolite LL presents the lowest *px* selectivity. This observation is consistent with the behavior observed in the previous section (inversion in the order of adsorption enthalpies between *px* and *ox*), therefore confirming that the LL morphology leads to lower adsorption energy for *px* molecules than the other samples.

Different interpretations for the loss in *px* selectivity for the hierarchical zeolites can be proposed. The first hypothesis is linked to the chemical nature of the external surface area which induce strong adsorption of the most polar xylene molecules (*mx* and *ox*) as compared to the apolar isomer *px*. Such a hypothesis indicates that large external surface areas provide additional adsorption sites. At high loading conditions, contrary to the microporous adsorption sites (mainly governed by entropic effects), such additional surface sites are expected to exhibit a different balance between the enthalpic and entropic adsorption contributions. However, such a hypothesis does not seem to fully explain the observed picture. Indeed, the decrease in *px* selectivity does not perfectly correlate with the external surface of NA zeolites. A second hypothesis concerning the loss in selectivity for the different hierarchical zeolites relates to morphology differences in the external surface for conventional and hierarchical zeolites. It is often stated that the selectivity towards *px* molecules in a conventional zeolite BaX is linked to a specific adsorption site – the so-called window site – at large adsorbed amounts [39,46,47]. Such a site only leads to the adsorption of *px* isomers as it corresponds to a preferential, aligned position of the methyl groups in *px* xylene isomer. Therefore, *px* leads to a larger number of favorable configurations when compared to other isomers. This suggests that *px* adsorption is entropically favored. In contrast, the impact of hierarchization on xylene adsorption in the window sites (which are selective to *px*) remains to be investigated. In practice, this adsorption site is located within zeolite windows that may be located at the exterior of the sample – i.e. at the crystal edges. Hierarchical solids with a significant outer surface area possess more edges compared to non-hierarchical zeolites. In the literature, it remains unclear I such open window sites at the external surface lead to the same *px* molecule adsorption (compared to that of a window site within the crystal). The important *px* selectivity difference between

hierarchical and conventional zeolites suggests that the loss in selectivity due to destabilized window sites is very plausible.

Decoupling Surface and Bulk Selectivity

The results are important findings. First, a higher capacity for xylene adsorption is observed for the NA hierarchical zeolites in comparison with the hierarchical zeolite LL and the conventional zeolite. However, in the same time, a loss in selectivity is observed for the hierarchical zeolites when compared with the data for the conventional faujasite. To provide a deeper understanding of xylene adsorption at the zeolite outer surface, we performed a molecular simulation study. In more detail, using Grand Canonical Monte Carlo simulations, the adsorbed amounts, selectivity and enthalpies of adsorption were evaluated for (i) a bulk zeolite (therefore containing only microporosity) and (ii) a zeolite possessing an external surface. The latter was obtained by cleaving the surface direction {011}. Choosing this surface allows investigating whether the presence of incomplete α cages on the surface of zeolites – more present in hierarchical zeolites – can impact selectivity (see section S2.4 of the supporting information).

The computed adsorption isotherms obtained using GCMC simulations are shown in Fig. 4 for pure xylene isomers in (i) a bulk zeolite crystal and (ii) a zeolite bearing an external surface. The number of adsorbed xylene molecules per α cage agrees with the experimental data reported above (as obtained at 175°C using gas phase experiments for a conventional zeolite). For *px*, the experimental adsorbed amount is ~3.5 molecules/α cage while the simulated adsorbed amount is 3.4 molecules/α cage for the bulk zeolite. Such a comparison allows validating the force field. The

simulated adsorption isotherms obtained for an equimolar mixture of xylene isomers are also displayed in Fig. 4. These binary simulations aim to check whether the employed model allows reproducing the affinity of the adsorbent for a given isomer. As can be seen from the data for the *px*/*mx* mixture, the amount of adsorbed *px* in the zeolite (dashed line) is significantly higher than that of *mx* (dotted line). This fact confirms the large *px* selectivity in the zeolite. The calculated selectivity at full loading is about 2.4, which is not far from the values available in the literature for similar systems; For a BaX zeolite, the *px*/*mx* selectivity is about 3 at 175°C in a equimolar mixture of the same isomers [21]. It is worth mentioning that the experimental selectivity is measured in a partially pre-hydrated BaX, which could explain the gain in selectivity compared to our system (since the latter does not account for the presence of water) [25].

As shown in Fig. 4, at high loadings and for the same given partial pressure, the simulated adsorbed amounts in the zeolite with an external surface are larger than those for the bulk zeolite. Such enhanced adsorption is thought to be linked to surface adsorption. When inspecting in detail the adsorption of each component of the equimolar mixture, two regions can be distinguished. At low loadings, an increase in *px* adsorption is observed with respect to *mx*. At larger loadings (above 3 molecules/α cage), a diminution in the *px* adsorbed amount is noticeable as the surface contribution comes into play.

To better assess the impact of the outer surface on the adsorption properties, a detailed investigation in terms of selectivity and adsorption enthalpy is required. In Fig. 5(a), a comparison between the adsorption selectivities (plotted as a function of loading) for the bulk zeolite and the

zeolite bearing an external surface is presented. As previously stated, in agreement with our experimental results, the simulation data indicate that the zeolite is *px* selective. The maximum *px* selectivity is observed beyond adsorption of the third xylene molecule. Such selectivity is due to the the large Ba cation volume as it induces adsorption of *px* in non-cationic sites at high loadings. This adsorption site (previously referred to as window site), which is only accessible to the *px* isomer, is located at the dodecagonal window center [39,46,47]. A maximum *px* selectivity ~3 can be observed in Fig. 5(a) for both zeolites (with and without external surface). This indicates that, upon adsorption of xylene, a maximum in the xylene isomer selectivity is attained close to saturation. However, beyond this maximum, a pronounced loss in selectivity is observed for the system involving adsorption at the external surface. Comparison between both data sets suggests that adsorption obeys a regime of surface selectivity once the maximum in selectivity is reached.

The density profiles for the adsorbed xylene isomers in the core of the zeolite and at its external surface were determined for the zeolite bearing an outer surface (Fig. 6). These density distributions are derived from the position of the xylene molecules in the direction perpendicular to the outer surface. Such histograms are normalized to the overall number of xylene adsorbed molecules so that they provide the adsorption probability at a distance z from the surface. Such density profiles are displayed in Fig. 6 for an equimolar binary mixture of *px*/*mx* adsorbed in the BaX zeolite (at different total pressures). For adsorption at low xylene pressure ($P = 5 \times 10^{-4}$ mbar), the adsorbed amount close to the surface is smaller than in the core of the zeolite. Even if the adsorbed amounts on the surface increases at higher pressures, the selectivity is also impacted by the pressure range and, consequently, by the loading. At high pressure ($P = 100$ mbar), when

significant surface adsorption occurs, the core of the zeolite close to the interface leads to a selectivity towards *px* that matches that observed for the bulk zeolite.

To better understand the effect of loading on surface adsorption, the selectivities associated to the different regions (bulk fluid, surface, and bulk crystal) were determined from the adsorption distribution profiles [see Fig. 5(b)]. In the first of the cases, as it is expected for a non-confined fluid, the non-selective region (representative of the meso/macroporosity) presents values close to one. It must be underlined that this contribution can only be determined for the higher loadings involving significant enough non-microporous adsorption. In the case of the second contribution (surface), the obtained results confirm that the surface selectivities are quite low (between 1-1.4) compared to the bulk crystal selectivity. Upon inspecting at the trend of the bulk crystal and surface selectivities, it is important to highlight that their values tend to converge (around 3.3 molecules/α cage) as the saturation is approached. Looking at Fig. S3 (density profiles for 3.3 molecules/α cage), this result might be explained by the fact that the surface behavior extends towards microporous regions – just beneath the external surface. Although probably this phenomenon is here overrepresented because of the limited system size, the observed trend confirms the importance of the confinement at the vicinity of the window site in the occurrence of para-selectivity. In the same direction, it is worth mentioning that the selectivity of the bulk crystal towards *px* is at least partially recovered when sufficient surface adsorption occurs. Thus, when the total filling of the non-selective region occurs, the adsorption mode on the surface carries a beneficial impact on para-selectivity. Such a picture is therefore expected to be more representative of batch experiments or liquid phase adsorption processes. Although the obtained values at higher adsorbed amounts do not reach the maxima observed for intermediate-high adsorbed amounts, the

extent of the observed phenomenon must be weighted depending on the amount of external surface.

Finally, the simulated isosteric enthalpies of adsorption for the bulk zeolite and the zeolite bearing an external surface are shown in Fig. 7. At low and intermediate adsorbed amounts, large adsorption enthalpies in BaX are observed due to the strong xylene/zeolite interactions. The adsorption enthalpies of adsorption found here are close to those reported in the literature (~120 kJ/mol in the case of BaX at 150°C) [45]. Contrary to the experimental adsorption enthalpies, which show a strong decrease in the adsorption enthalpy at high adsorbed amounts, this phenomenon is not detected through simulation for the bulk zeolite. The absence of such behavior, which is typical of systems showing significant surface condensation, is due to the absence of outer surface in simulations for bulk zeolites. Since this is not anymore the case for the system incorporating the interface, the change in the adsorption enthalpies matches those reported elsewhere [19]. In such data, the adsorption enthalpies significantly decrease at high adsorbed amounts. We note the correlation between the adsorption enthalpies and selectivity. For the BaX zeolite bearing an external surface, our data suggest that the decrease in the adsorption enthalpy at high loadings is related to the bulk/surface transition observed for the selectivity results.

4. Conclusions

The capacity towards xylene adsorption obtained for the different hierarchical zeolites using thermogravimetry indicate higher adsorbed amounts for NA hierarchical zeolites (compared to the results obtained for a conventional zeolite). In contrast, xylene adsorption observed with an LL

hierarchical zeolite is found to be comparable or smaller than for the conventional zeolite. To investigate xylene separation close to the saturation regime, the isosteric adsorption enthalpies were derived from the adsorbed amounts obtained for pure xylene isomers in the hierarchical and conventional zeolites. The adsorption enthalpies for the *px* and *ox* isomers are very close, therefore suggesting the absence of possible enthalpic effects due to surface selectivity.

With respect to the conventional zeolite, hierarchical zeolites exhibit a loss in *px* selectivity. Such a selectivity loss is thought to be linked to the stability decrease of the *px* selective window sites at large adsorbed amounts. Such a site, which is located at the 12-membered-ring window center, has been already proposed as responsible for *px* selectivity in BaX zeolites [39,40]. Moreover, it can be proposed that the presence of an increased external surface area (like in hierarchical zeolites) can induce a decrease of the stability of *px* adsorption in these window sites. This would explain the marked selectivity loss for the NA-3 zeolite, which displays the largest outer surface area among the hierarchical zeolites considered here. Despite a smaller outer surface area in the case of the LL zeolite (compared to the NA-3 zeolite), the selectivity for both hierarchical zeolites are of the same order. This indicates that the layer-like crystal morphology in the LL zeolite also induces a loss in xylene selectivity.

The molecular simulation carried out using the Monte Carlo method in the Grand Canonical ensemble confirms an adsorption increase due to the external surface. The experimental *px* selectivity loss at the outer surface is confirmed by our Monte Carlo simulations. Such a selectivity loss, induced by the presence of the external surface, is about 30%. A reduction of the selectivity

was observed for a model taking into account the surface {011}, whose cutting-plane crosses the α cages and, hence, generates incomplete dodecagonal windows at the surface. This fact is in agreement with the hypothesis that the observed loss of *px* selectivity is related to the presence of likely incomplete α cages at the external surface in hierarchical zeolites.

Appendix A. Supplementary data

Supplementary data to this article can be found online at doi.XXX

References

[1]   Y. Yang, P. Bai, X. Guo, Separation of Xylene Isomers: A Review of Recent Advances in Materials, Ind. Eng. Chem. Res. 56 (2017) 14725–14753. doi:10.1021/acs.iecr.7b03127.

[2]   Y.F. Yeong, A.Z. Abdullah, A.L. Ahmad, S. Bhatia, Separation of p-xylene from binary xylene mixture over silicalite-1 membrane: Experimental and modeling studies, Chem. Eng. Sci. 66 (2011) 897–906. doi:10.1016/j.ces.2010.11.035.

[3]   S. Mintova, J.P. Gilson, V. Valtchev, Advances in nanosized zeolites, Nanoscale. 5 (2013) 6693–6703. doi:10.1039/c3nr01629c.

[4]   M. Khaleel, A.J. Wagner, K.A. Mkhoyan, M. Tsapatsis, On the rotational intergrowth of hierarchical FAU/EMT zeolites, Angew. Chemie - Int. Ed. 53 (2014) 9456–9461. doi:10.1002/anie.201402024.

[5]   A. Inayat, I. Knoke, E. Spiecker, W. Schwieger, Assemblies of mesoporous FAU-type zeolite nanosheets, Angew. Chemie - Int. Ed. 51 (2012) 1962–1965. doi:10.1002/anie.201105738.

[6]   J. García-Martínez, M. Johnson, J. Valla, K. Li, J.Y. Ying, Mesostructured zeolite y - High hydrothermal stability and superior FCC catalytic performance, Catal. Sci. Technol. 2 (2012) 987–994. doi:10.1039/c2cy00309k.

[7]   D. Mehlhorn, A. Inayat, W. Schwieger, R. Valiullin, J. Kärger, Probing mass transfer in mesoporous faujasite-type zeolite nanosheet assemblies, ChemPhysChem. 15 (2014) 1681–1686. doi:10.1002/cphc.201301133.

[8]   V. P. Valtchev, K. N. Bozhilov, Transmission Electron Microscopy Study of the Formation of FAU-Type Zeolite at Room Temperature, J. Phys. Chem. B. 108 (2004) 15587–15598. doi:10.1021/jp048341c.

[9]   A. Galarneau, F. Guenneau, A. Gedeon, D. Mereib, J. Rodriguez, F. Fajula, B. Coasne, Probing Interconnectivity in Hierarchical Microporous/Mesoporous Materials Using Adsorption and Nuclear Magnetic Resonance Diffusion, J. Phys. Chem. C. 120 (2016) 1562–1569. doi:10.1021/acs.jpcc.5b10129.

[10]   B. Coasne, Multiscale adsorption and transport in hierarchical porous materials, New J. Chem. 40 (2016) 4078–4094. doi:10.1039/c5nj03194j.

[11]   I.I. Ivanova, E.E. Knyazeva, Micro-mesoporous materials obtained by zeolite recrystallization: Synthesis, characterization and catalytic applications, Chem. Soc. Rev. 42 (2013) 3671–3688. doi:10.1039/c2cs35341e.

[12]   Y. Ren, Z. Ma, R.E. Morris, Z. Liu, F. Jiao, S. Dai, P.G. Bruce, A solid with a hierarchical tetramodal micro-meso-macro pore size distribution, Nat. Commun. 4 (2013) 1–7. doi:10.1038/ncomms3015.

[13]   G.J. de A.A. Soler-Illia, C. Sanchez, B. Lebeau, J. Patarin, Chemical Strategies To Design Textured Materials: from Microporous and Mesoporous Oxides to Nanonetworks and Hierarchical Structures, Chem. Rev. 102 (2002) 4093–4138. doi:10.1021/cr0200062.

[14]   D. Verboekend, S. Mitchell, J. Pérez-Ramírez, Hierarchical Zeolites Overcome all Obstacles: Next Stop Industrial Implementation, Chim. Int. J. Chem. 67 (2013) 327–332. doi:10.2533/chimia.2013.327.

[15]   S. Mitchell, N.L. Michels, K. Kunze, J. Pérez-Ramírez, Visualization of hierarchically structured zeolite bodies from macro to nano length scales, Nat. Chem. 4 (2012) 825–831. doi:10.1038/nchem.1403.

[16]   J.-P. Bellat, M.-H. Simonot-Grange, Adsorption of gaseous p-xylene and m-xylene on NaY, KY, and BaY zeolites. Part 2: Modeling. Enthalpies and entropies of adsorption, Zeolites. 15 (1995) 219–227. doi:10.1016/0144-2449(94)00048-W.

[17]   J.P. Bellat, M.H. Simonot-Grange, S. Jullian, Adsorption of gaseous p-xylene and m-xylene on NaY, KY, and BaY zeolites: Part 1. Adsorption equilibria of pure xylenes, Zeolites. 15 (1995) 124–130. doi:10.1016/0144-2449(94)00030-V.

[18]   V. Cottier, J.-P. Bellat, M.-H. Simonot-Grange, A. Méthivier, Adsorption of p-Xylene/m-Xylene Gas Mixtures on BaY and NaY Zeolites. Coadsorption Equilibria and Selectivities, J. Phys. Chem. B. 101 (1997) 4798–4802. doi:10.1021/jp9640033.

[19]   C. Pichon, A. Méthivier, M.-H. Simonot-Grange, Adsorption of m-Xylene on Prehydrated Zeolite BaX: Correlation between Temperature-Programmed Desorption and Low-Temperature Neutron Powder Diffraction Studies, Langmuir. 16 (1999) 1931–1936. doi:10.1021/la990819u.

[20]   D.M. Ruthven, M. Goddard, Sorption and diffusion of C8 aromatic hydrocarbons in faujasite type zeolites. I. Equilibrium isotherms and separation factors, Zeolites. 6 (1986) 275–282. doi:10.1016/0144-2449(86)90081-3.

[21]   H. Tournier, A. Barreau, B. Tavitian, D. Le Roux, J.-C. Moïse, J.-P. Bellat, C. Paulin, Adsorption Equilibrium of Xylene Isomers and p-Diethylbenzene on a Prehydrated BaX Zeolite, Ind. Eng. Chem. Res. 40 (2001) 5983–5990. doi:10.1021/ie0011371.

[22]   M.H. Simonot-Grange, O. Bertrand, E. Pilverdier, J.P. Bellat, C. Paulin, Differential calorimetric enthalpies of adsorption of p-xylene and m-xylene on Y faujasites at 25° C, J. Therm. Anal. 48 (1997) 741–754. doi:10.1007/BF01997180.

[23]   X. Yan, S. Komarneni, Z. Yan, CO2 adsorption on Santa Barbara Amorphous-15 (SBA-15) and amine-modified Santa Barbara Amorphous-15 (SBA-15) with and without controlled microporosity, J. Colloid Interface Sci. 390 (2013) 217–224. doi:10.1016/J.JCIS.2012.09.038.

[24]   J.P. Bellat, E. Pilverdier, M.H. Simonot-Grange, S. Jullian, Microporous volume and external surface of Y zeolites accessible to p-xylene and m-xylene, Microporous Mater. 9 (1997) 213–220. doi:10.1016/S0927-6513(96)00108-3.

[25]   J.-C. Moïse, Equilibres de coadsorption du p-xylène et du m-xylène par les zéolithes X et Y. Effet du cation compensateur, de la température et du taux d'hydratation de la zéolithe sur la sélectivité d'adsorption, 1999. http://www.theses.fr/1999DIJOS069.

[26]   M. Minceva, A.E. Rodrigues, Adsorption of Xylenes on Faujasite-Type Zeolite: Equilibrium and Kinetics in Batch Adsorber, Chem. Eng. Res. Des. 82 (2004) 667–681. doi:10.1205/026387604323142739.

[27]   R.M. Moore, J.R. Katzer, Counterdiffusion of liquid hydrocarbons in type Y zeolite: Effect of molecular size, molecular type, and direction of diffusion, AIChE J. 18 (1972) 816–824. doi:10.1002/aic.690180426.

[28]   V. Moya-Korchi, Etude de la contre-diffusion des xylenes dans des adsorbants zeolithiques de type y, 1995. http://www.theses.fr/1995PA066410.

[29]   M.S.P. Silva, M.A. Moreira, A.F.P. Ferreira, J.C. Santos, V.M.T.M. Silva, P. Sá Gomes, M. Minceva, J.P.B. Mota, A.E. Rodrigues, Adsorbent Evaluation Based on Experimental Breakthrough Curves: Separation of p-Xylene from C8 Isomers, Chem. Eng. Technol. 35 (2012) 1777–1785. doi:10.1002/ceat.201100672.

[30]   Y. Khabzina, C. Laroche, J. Perez-Pellitero, D. Farrusseng, Xylene separation on a diverse library of exchanged faujasite zeolites, Microporous Mesoporous Mater. 247 (2017) 52–59. doi:10.1016/J.MICROMESO.2017.03.026.

[31]   M.S.P. Silva, J.P.B. Mota, A.E. Rodrigues, Fixed-bed adsorption of aromatic C8 isomers: Breakthrough experiments, modeling and simulation, Sep. Purif. Technol. 90 (2012) 246–256. doi:10.1016/J.SEPPUR.2012.02.034.

[32]   F. Awum, S. Narayan, D. Ruthven, Measurement of intracrystalline diffusivities in NaX zeolite by liquid chromatography, Ind. & Eng. Chem. Res. 27 (2002) 1510–1515. doi:10.1021/ie00080a027.

[33]   I.C. Medeiros-Costa, C. Laroche, J. Pérez-Pellitero, B. Coasne, Characterization of hierarchical zeolites: Combining adsorption/intrusion, electron microscopy, diffraction and spectroscopic techniques, Microporous Mesoporous Mater. 287 (2019) 167–176. doi:10.1016/j.micromeso.2019.05.057.

[34]   Materials Studio. Dassault Systèmes BIOVIA: San Diego, (n.d.).

[35]   J. C. Crabtree, M. Molinari, S. C. Parker, J. A. Purton, Simulation of the Adsorption and Transport of CO2 on Faujasite Surfaces, J. Phys. Chem. C. 117 (2013) 21778–21787. doi:10.1021/jp4053727.

[36]   B. Coasne, A. Galarneau, C. Gerardin, F. Fajula, F. Villemot, Molecular Simulation of Adsorption and Transport in Hierarchical Porous Materials, Langmuir. 29 (2013) 7864–7875. doi:10.1021/la401228k.

[37]   C. Nieto-Draghi, P. Bonnaud, P. Ungerer, Anisotropic United Atom Model Including the Electrostatic Interactions of Methylbenzenes. I. Thermodynamic and Structural Properties, J. Phys. Chem. C. 111 (2007) 15686–15699. doi:10.1021/jp0737146.

[38]   P. Pascual, P. Ungerer, B. Tavitian, P. Pernot, A. Boutin, Development of a transferable guest–host force field for adsorption of hydrocarbons in zeolites I. Reinvestigation of alkane adsorption in silicalite by grand canonical Monte Carlo simulation, Phys. Chem. Chem. Phys. 5 (2003) 3684–3693. doi:10.1039/B304209J.

[39]   V. Lachet, Simulation moleculaire de l'adsorption selective des isomeres du xylene dans les faujasites, 1998.

[40]   A. Descours, Adsorption des isomeres para- et méta- du xylène dans les zeolithes NaX et BaX : étude des relations propriétés-structure, 1997. http://www.theses.fr/1997DIJOS012.

[41]   M. Polanyi, Section III.—Theories of the adsorption of gases. A general survey and some additional remarks. Introductory paper to section III, Trans. Faraday Soc. 28 (1932) 316–333. doi:10.1039/TF9322800316.

[42]   S.J. Gregg, K.S.W. Sing, Adsorption, surface area, and porosity, 2nd ed, Academic Press, Great Britain, 1995. https://books.google.fr/books?id=YhNRAAAAMAAJ.

[43]   N.D. Hutson, R.T. Yang, Theoretical basis for the Dubinin-Radushkevitch (D-R) adsorption isotherm equation, Adsorption. 3 (1997) 189–195. doi:10.1007/BF01650130.

[44]   F. Villemot, A. Galarneau, B. Coasne, Adsorption and Dynamics in Hierarchical Metal–Organic Frameworks, J. Phys. Chem. C. 118 (2014) 7423–7433. doi:10.1021/jp500037z.

[45]   C. Mellot, M.H. Simonot-Grange, E. Pilverdier, J.P. Bellat, D. Espinat, Adsorption of Gaseous p- or m-Xylene in BaX Zeolite: Correlation between Thermodynamic and Crystallographic Studies, Langmuir. 11 (1995) 1726–1730. doi:10.1021/la00005a049.

[46]   C. Pichon, Etude structurale et énergétique de l'adsorption des isomères para- et méta- du xylène dans la zéolithe BaX préhydratée : caractérisation par diffraction des neutrons et thermodésorption programmée, 1999. http://www.theses.fr/1999DIJOS051.

[47]   C. Mellot-Drazniecks, Caracterisation structurale de l'adsorption des isomeres para- et meta- du xylene dans des zeolithes de type faujasite, 1993. http://www.theses.fr/1993PA066608.

Table 1. Textural parameters of BaX conventional and hierarchical zeolites (adapted from Ref.[33]): Micropore volume V_μ, mesoporous volume V_{meso}, and outer surface area S_{ext} of nanoparticles aggregates (NA), layer-like (LL) and conventional (Conv.) zeolites are presented. The conventional zeolite is a BaX zeolite obtained by Baryum cationic exchange of commercial Siliporite G5 from CECA-Arkema.

| Sample	$V_\mu(cm^3/g)$	$S_{ext}(m^2/g)$	$V_{meso}(cm^3/g)$
NA-1	0.18	43	0.11
NA-2	0.16	48	0.13
NA-3	0.16	68	0.18
LL	0.18	38	0.08
Conv.	0.25	11	0.01

Table 2. Xylene adsorption data after 3h and 24 h for the hierarchical and conventional zeolites at room temperature. The xylene adsorption capacities are expressed in molecules/α cage, accounting for the total adsorption (*px* + *ox*). *px*/*ox* selectivities are also presented for each zeolite after 3 and 24 h. *Remaining adsorbed amounts for nC10 upon xylene adsorption are also shown.

px/ox	3h			24h		
Sample (BaX)	Molecules/ α Cage	*nC10 (g)	Selectivity (px/ox)	Molecules/ α Cage	*nC10 (g)	Selectivity (px/ox)
NA-1	2.75	0.09	1.75	3.14	0.06	1.89
NA-2	2.92	0.06	1.87	3.16	0.05	2.35
NA-3	3.10	0.06	1.49	3.21	0.05	1.62
LL	2.33	0.12	1.37	2.56	0.10	1.54
Conv.	1.92	0.20	1.50	2.66	0.13	3.71

Table 3. Xylene (*px* + *mx*) adsorption data after 3h and 24 h for the hierarchical and conventional zeolites at room temperature. The xylene adsorption capacities are expressed in molecules/α cage, accounting for the total adsorption (*px* + *mx*). *px*/*mx* selectivities are also presented for each zeolite after 3 and 24 h. *Remaining adsorbed amounts of nC10 upon xylene adsorption are also shown.

px/mx	3h	24h

Sample (BaX)	Molecule /α Cage	*nC10 (g)	Selectivity (px/mx)	Molecule /α Cage	*nC10 (g)	Selectivity (px/mx)
NA-1	2.51	0.11	1.61	3.32	0.05	1.79
NA-2	2.65	0.09	1.85	2.87	0.07	2.17
NA-3	2.89	0.07	1.34	3.07	0.06	1.36
LL	2.41	0.12	1.23	2.57	0.10	1.31
Conv.	1.85	0.21	1.72	2.87	0.11	2.67
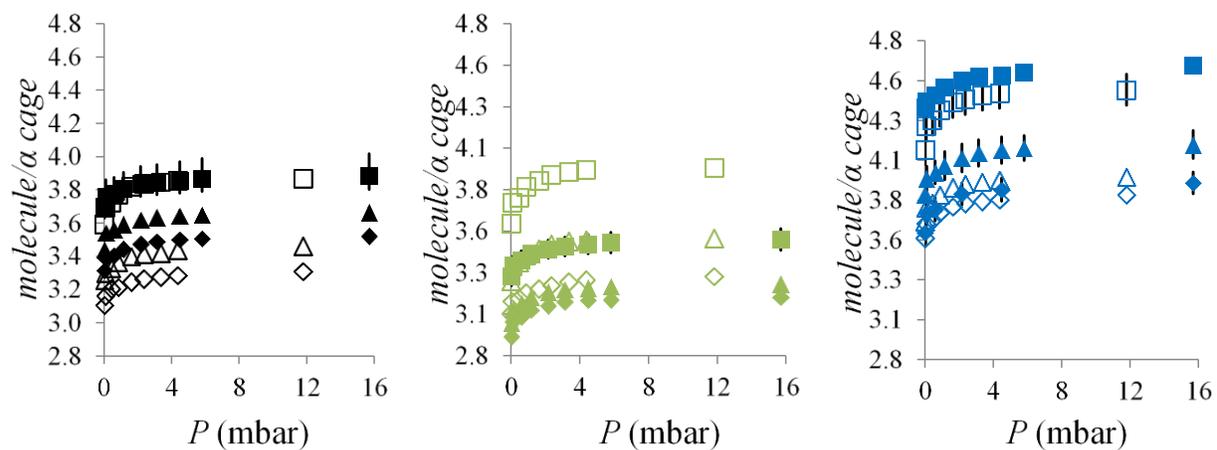
Figure 1. (color online) Single component adsorption isotherms for *px* and *ox* in hierarchical and conventional BaX zeolites: Conventional (black), LL (green) and NA-3 (blue). Filled symbols correspond to *px* adsorption while empty symbols correspond to *ox* adsorption. The temperatures are indicated by the symbols: squares (100°C), triangles (150°C) and diamonds (175°C).
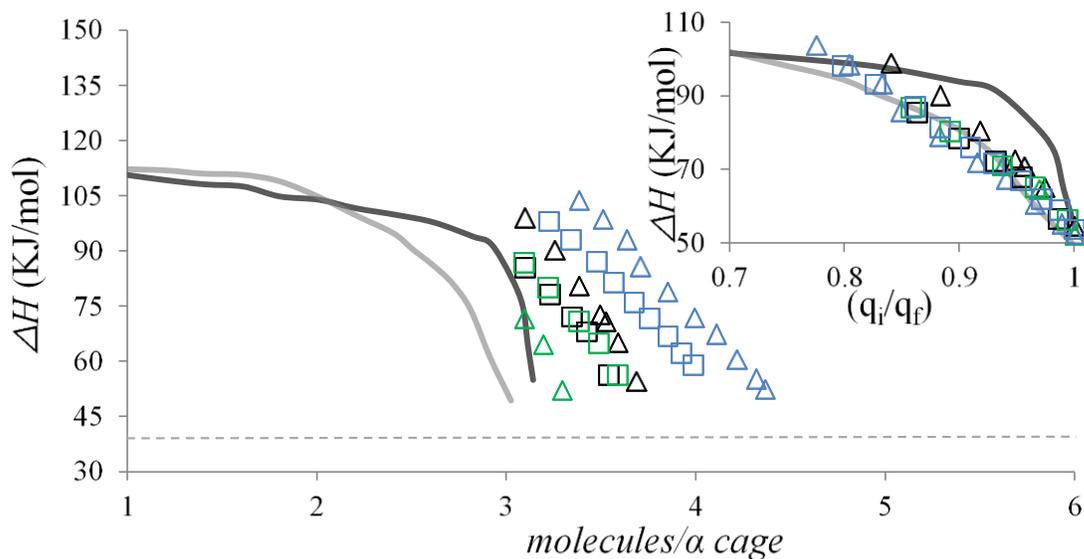
Figure 2. (color online) Isosteric adsorption enthalpies at 150°C of xylenes in BaX zeolite as a function of the number of molecules per cage and fractional loading q_i/q_f (inset). The triangles and squares represent the enthalpies of adsorption of pure *px* and *ox*, respectively. The black symbols correspond to the data for the conventional BaX zeolite while the green and blue symbols are those for LL and NA-3 hierarchical zeolites, respectively. The solid lines represent adsorption enthalpies data available in the literature: adsorption enthalpies of *mx* (dark grey) and *px* (light grey) in BaX at 150°C.[45] The dashed line indicates the enthalpy of vaporization at the same temperature.
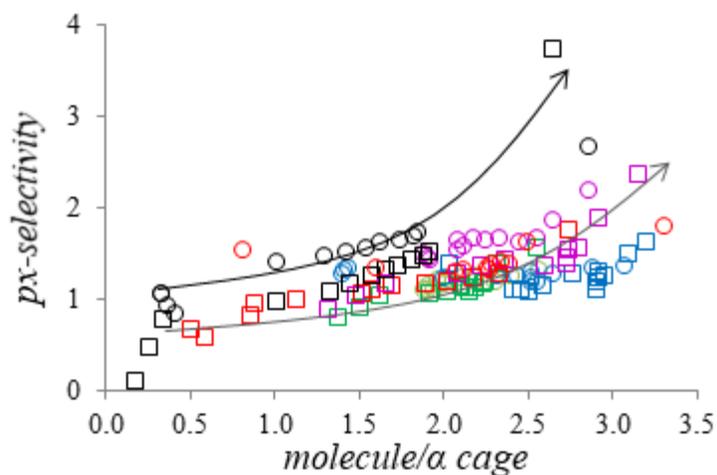
Figure 3. (color online) *px* isomer selectivity at different adsorbed amounts for conventional zeolites (black) and hierarchical zeolites: NA-1 (red), NA-2 (purple), NA-3 (blue) and LL (green). The squares are for *px/ox* selectivities while the circles are for *px/mx* selectivities. These tests were performed at ambient temperature in excess of nC10 and subsequent addition of *px/mx* (50%:50%). The arrows are guides to the eye to illustrate the selectivity trend for conventional (black) and hierarchical (gray) zeolites.
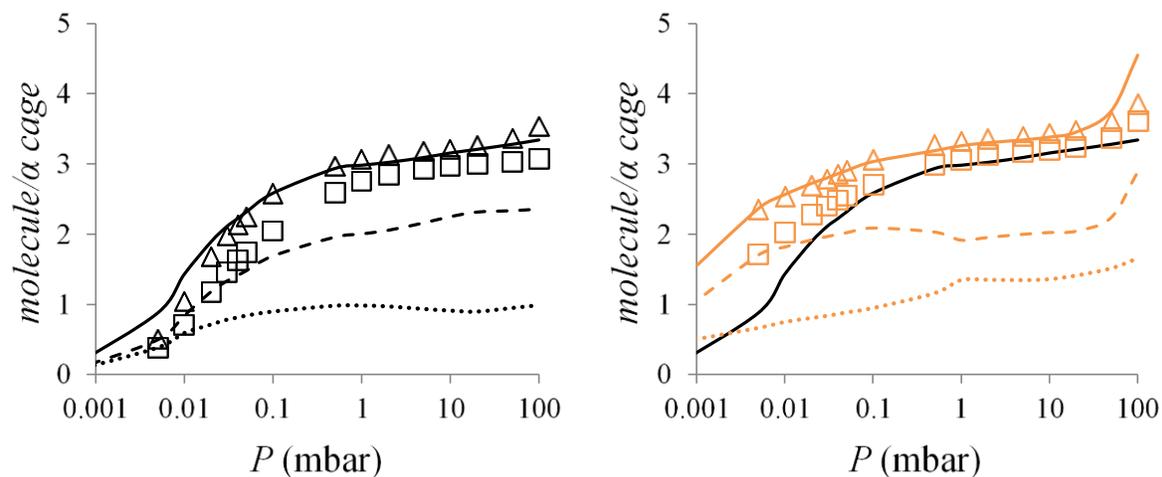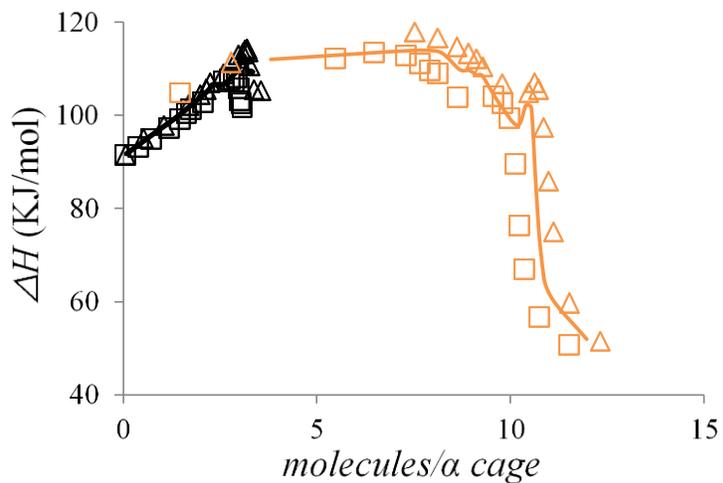
Figure 4. (color online) Simulated xylene adsorption isotherms at 175°C in a bulk Ba zeolite (left) and in a Ba zeolite bearing an external surface (right). The single component adsorption isothems for xylene isomers are represented by the symbols: *px* (triangles) and *mx* (squares). The co-adsorption isotherm for the *px*/*mx* mixture corresponds to the solid line. The adsorbed amounts for each isomer in the mixture correspond to the dashed (*px*) and dotted (*mx*) lines. For comparison, in the right-hand graph, the solid black line shows the *px*/*mx* adsorbed amounts in the bulk zeolite.
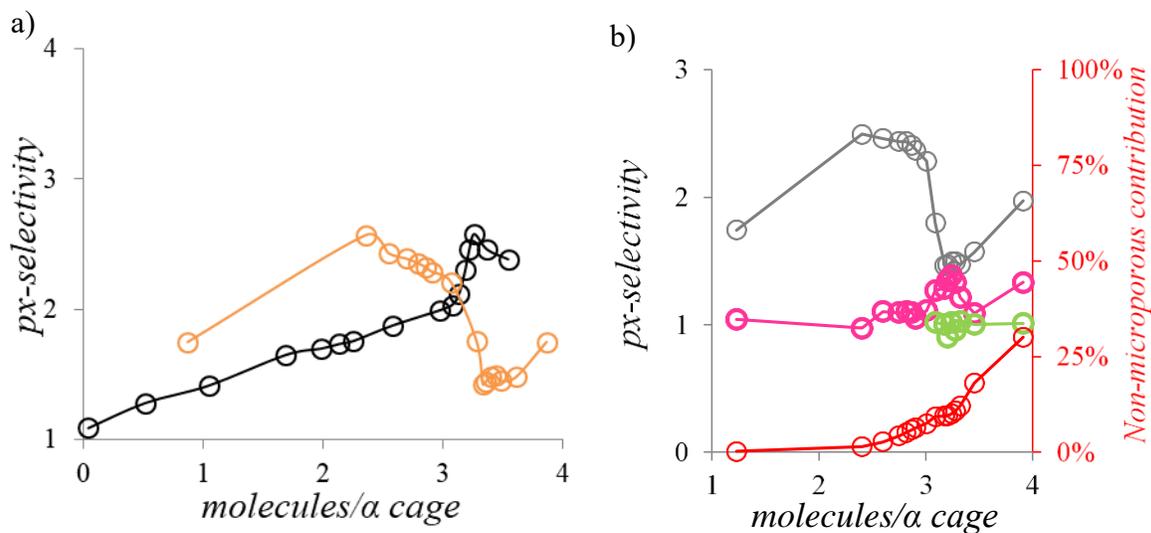
Figure 5. (color online) a) *px* selectivity in the bulk zeolite (black) and in the zeolite with an external surface (orange) versus the adsorbed amount in molecules per α cage. The *px* isomer selectivities were derived at 175°C from the adsorption isotherms for the *px*/*mx* mixture reported in Figure 4. b) *px* selectivities for the bulk crystal (gray), surface (pink) and bulk fluid (green). *px* selectivities must be read on the left vertical axis. The surface and bulk fluid contributions to the total adsorption data are represented by the red curve with values on the right vertical axis.
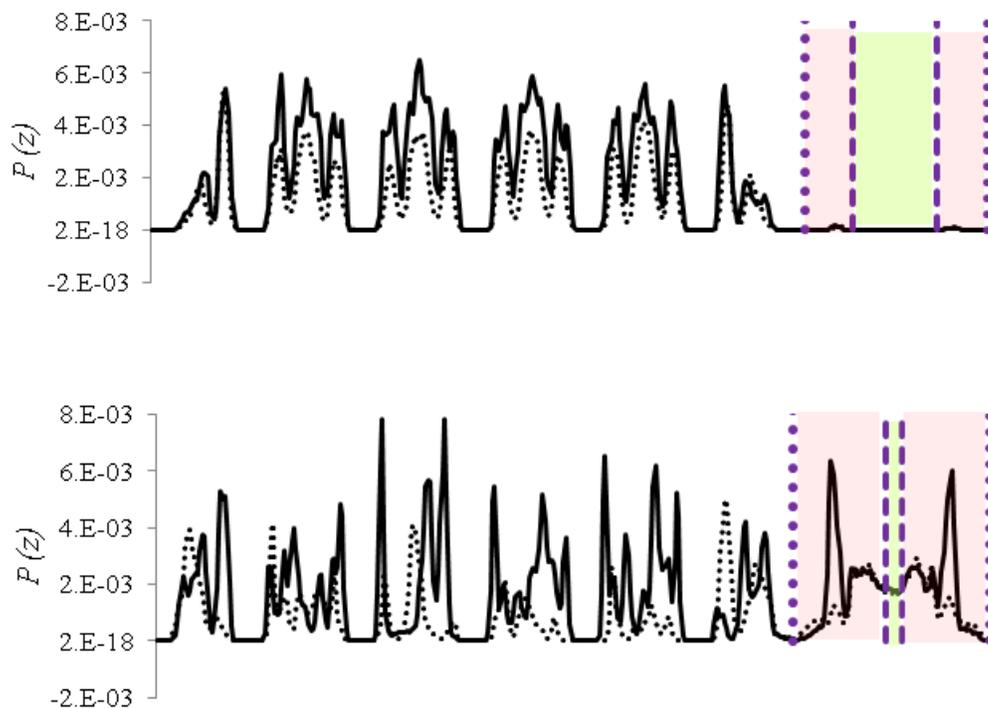
Figure 6. (color online) Simulated density profiles for *px* (solid line) and *mx* (dotted line) isomers as determined upon adsorption at 175°C of an equimolar binary mixture in a BaX zeolite bearing an outer surface. The overall pressures and corresponding loadings are: $P = 5 \times 10^{-4}$ mbar and 1.3 molecules/α cage (top); 100 mbar and 3.9 molecules/α cage (bottom). Green and pink regions represent the bulk and surface fluid regions, respectively. The dotted and dashed purple lines account for the bulk crystal/surface and surface/bulk fluid interfaces, respectively. Distribution profiles at intermediate pressures/loadings are present in Fig. S3.

Figure 7. (color online) Simulated isosteric adsorption enthalpies for xylene isomers at 175°C in bulk BaX zeolite (black) and in a BaX zeolite with an external surface (orange). The data for pure xylene isomers corresponds to the different symbols: *px* (triangles) and *mx* (squares). The adsorption enthalpy for an equimolar *px*/*mx* mixture is indicated by the solid line.